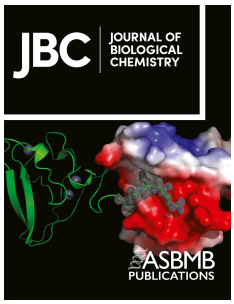

Cellular and functional insights into FIH-mediated hydroxylation of TRPA1

Tao Guo, Dianne Marquez Lopez, Siyuan Wang, Liudi Yao, Xi Li, Elizabeth R. Davies, Mariana Vargas-Caballero, Nullin Divecha, Christopher J. Schofield, Katrin Deinhardt, Yihua Wang

PII: S0021-9258(25)02734-6

DOI: https://doi.org/10.1016/j.jbc.2025.110882

Reference: JBC 110882

To appear in: *Journal of Biological Chemistry*

Received Date: 1 July 2025

Revised Date: 22 September 2025

Accepted Date: 25 October 2025

Please cite this article as: Guo T, Lopez DM, Wang S, Yao L, Li X, Davies ER, Vargas-Caballero M, Divecha N, Schofield □□□□□□□□□ CJ, Deinhardt K, Wang Y, Cellular and functional insights into FIH-mediated hydroxylation of TRPA1, *Journal of Biological Chemistry* (2025), doi: https://doi.org/10.1016/j.jbc.2025.110882.

Cellular and functional insights into FIH-mediated hydroxylation of TRPA1

Tao Guo[1,#], Dianne Marquez Lopez[1,7,#], Siyuan Wang[1,#], Liudi Yao[1], Xi Li[1], Elizabeth R. Davies[1,2], Mariana Vargas-Caballero[1,3], Nullin Divecha[1,3], Christopher J. Schofield[4], Katrin Deinhardt[1,3,5]*, and Yihua Wang[1,3,6]*

[1]Biological Sciences, Faculty of Environmental and Life Sciences, University of Southampton, Southampton SO17 1BJ, U.K.

[2]Clinical and Experimental Sciences, Faculty of Medicine, University of Southampton, Southampton SO16 6YD, U.K.

[3]Institute for Life Sciences, University of Southampton, Southampton SO17 1BJ, UK.

[4]Department of Chemistry and the Ineos Oxford Institute for Antimicrobial Research, Chemistry Research Laboratory, Mansfield Road, University of Oxford, Oxford OX1 3TA, U.K.

[5]University of Bremen, Cell Biology, 28359 Bremen, Germany

[6]NIHR Southampton Biomedical Research Centre, University Hospital Southampton, Southampton SO16 6YD, U.K.

[7]UK Dementia Research Institute, Centre for Discovery Brain Sciences, University of Edinburgh, Edinburgh Bioquarter, Edinburgh EH16 4SB, U.K.

[#]These authors contributed equally.

*Correspondence to: yihua.wang@soton.ac.uk or kdeinhar@uni-bremen.de

Keywords: Transient Receptor Potential (TRP) channel, ankyrin, hypoxia inducible factor HIF, factor inhibiting HIF (FIH), post translational modification / hydroxylation.

Abstract

Transient receptor potential cation channel, subfamily A, member 1 (TRPA1), also known as transient receptor potential ankyrin 1, is an ion channel located on the plasma membrane of cells. It is best known as a sensor for pain, cold, and itch in humans and other mammals, as well as for detecting electrophilic sensory irritants, including allyl isothiocyanate (AITC). A previous study confirmed that TRPA1 undergoes hydroxylation at Asn336 by the 2-oxoglutarate oxygenase Factor Inhibiting Hypoxia Inducible Factor (FIH). However, the biological significance of this modification remains unclear. Here, we present cellular and functional studies on the consequences of FIH-mediated asparaginyl hydroxylation of TRPA1. Co-immunoprecipitation experiments indicate that TRPA1 interacts with FIH in cells, in a manner likely involving the FIH dimer interface, as demonstrated by studies with the L340R FIH variant, which is unable to dimerize. Functional studies further suggest that FIH-mediated hydroxylation may be linked to AITC-induced channel activation. This response is diminished or delayed in TRPA1-expressing HEK 293T cells and absent in primary hippocampal cultures when FIH activity is lacking. These findings highlight a potential new avenue for the therapeutic manipulation of TRPA1.

Introduction

Transient receptor potential cation channel, subfamily A, member 1 (TRPA1), also known as transient receptor potential ankyrin 1, is a member of the transient receptor potential channel family (1). As a non-selective cation channel that is predominantly permeable to calcium (Ca^{2+}), TRPA1 can be activated by a number of reactive and non-reactive compounds and is thus considered as a "chemosensor". In addition to sensory neurons (2), TRPA1 is expressed in hippocampal and cortical neurons (3) where it alters electrophysiological properties of action potentials (4). Allyl isothiocyanate (AITC) potently activates TRPA1 (5) via covalent modification of a key cysteine residue within its *N*-terminal cytosolic domain (6).

Evidence has also been reported suggesting that TRPA1 may function in a manner related to oxygen/hypoxia sensing (7, 8). TRPA1 channel activity has been reported to be regulated by the catalytic activity of Hypoxia Inducible Factor (HIF)-α prolyl hydroxylases (7). However, the prolyl hydroxylation of TRPA1 in cells requires further validation as a subsequent study has shown lack of activity of recombinant Prolyl Hydroxylase Domain protein (PHD)1-3 on reported non-HIF substrates, including TRPA1 (9). By contrast, Saward *et al*. have shown that Factor Inhibiting HIF (FIH) can catalyse hydroxylation of TRPA1 at asparagine (Asn, N) 336 within an ankyrin repeat domain (ARD) (10), although the biological significance of this modification remains unclear.

FIH, encoded by the *HIF1AN* gene, is a Fe (II)- and 2-oxoglutarate-dependent dioxygenase, which classically acts as a negative regulator of HIF activity. FIH regulates HIF activity via hydroxylating a conserved Asn residue within the C-terminal activation domain (CAD) of HIF-1/2α, a post-translational modification that blocks interactions between the HIFα-CAD and CBP/p300 (11-17). FIH has multiple non-HIF

substrates, including members of the ARD protein family consistent with roles beyond those of HIF regulation (18-24). Either via HIF-dependent and / or HIF-independent pathways, FIH has been reported to regulate metabolism (25-29), keratinocyte differentiation (30), vascular endothelial cell survival (31), lung tissue stiffness (32), tumour growth (33-35) and metastasis (36) as well as Wnt signalling (37).

Here, we present cellular and functional investigations on the role of FIH catalysed hydroxylation of TRPA1, the results of which suggest that FIH-mediated hydroxylation may be linked to AITC-induced channel activation.

Results

TRPA1 binding to FIH involves the dimer interface

We initially tested for interaction between FIH and TRPA1 using co-immunoprecipitation experiments. Genes encoding for wild-type (WT) hemagglutinin (HA) tagged-FIH and HA-FIH variants with WT V5-TRPA1 were overexpressed in a human embryonic kidney (HEK) 293T cell 'FIH CRISPR knock-out' subline (FIH KO 293T) with subsequent co-precipitation of HA-FIH. HA-FIH variants investigated included a catalytically inactive D201A variant and the L340R FIH variant, which, at least in some contexts, fails to dimerize (38). Interestingly, the L340R FIH variant showed increased co-immunoprecipitation of V5-TRPA1 compared to the WT FIH and D201A HA-FIH (Figure 1; $P < 0.05$).

Effects of FIH-mediated hydroxylation of TRPA1 on AITC-induced channel activation in TRPA1-expressing HEK 293T cells

The TRPA1 agonist AITC increases intracellular calcium ion concentrations in cells expressing TRPA1 in a concentration-dependent manner (39). To investigate whether FIH-catalysed hydroxylation of TRPA1 affects AITC-induced channel activation, WT and FIH KO HEK 293T cells were transfected with a vector encoding WT human TRPA1 and a fluorescent calcium sensor protein (GCaMP) (40) (Figure 2A). We observed rapid changes in GCaMP fluorescence in WT TRPA1-expressing cells upon the application of AITC (Figure 2B). Notably, a slow increase in GCaMP fluorescence was observed in FIH KO 293T cells expressing WT TRPA1 (Figure 2B). To investigate the role of TRPA1 hydroxylation at N336, WT and FIH KO 293T cells were transfected with a vector encoding the hydroxylation-deficient TRPA1-N336A mutant (Figure 2A). In each case, we observed that the increase in GCaMP fluorescence in response to

AITC was eliminated (Figure 2B). These observations suggest that FIH-mediated interaction with N336, including hydroxylation, may regulate TRPA1 sensitivity towards AITC.

Effects of FIH inhibition on AITC-induced channel activation in murine hippocampal cultures

TrpA1 is expressed in neurons of the central nervous system, including hippocampal cultures (Figure 3A; Figure 5A) (3), where it modulates neuronal activity (4). We detected FIH (*Hif1an*) mRNA expression in hippocampal, cortical, striatal and dorsal root ganglia (DRG) cultures (Figure 3A). The presence and functional role of Trpa1 in hippocampal cultures were further validated using AITC and HC-030031, a well-characterized and selective Trpa1 antagonist (41). Application of AITC, but not DMSO (Figures 3B), significantly increased neuronal activity (Figures 3C; $P = 0.0140$), and this response was abolished by HC-030031 (Figure 3D; $P > 0.05$).

To assess whether FIH affects neuronal activity in hippocampal cultures, we grew cells in the presence of a prodrug form of the the FIH-selective inhibitor *N*-oxalyl-*D*-phenylalanine, that is dimethyl *N*-oxalyl-*D*-phenylalanine (DM-NOFD) (32, 42) for 14 days prior to calcium imaging as a read-out of neuronal activity. Cultures grown in the inhibitor remain viable and indistinguishable by gross morphology from their untreated counterparts (Supplementary Figure 1). Growing cultures in the absence of active FIH increased the baseline frequency of Ca^{2+} transients (Figures 4; $P = 0.0069$). Addition of AITC to activate Trpa1 lead to a significant increase in neuronal activity compared to vehicle-treated hippocampal cultures (Figures 4; $P = 0.0068$). Under conditions of FIH inhibition (DM-NOFD) cultures showed an enhanced level of baseline excitability measured as GCaMP transient frequency. Trpa1 activation with AITC did not further

increase the frequency of these Ca^{2+} transients when FIH was inhibited (Figures 4; *P* = 0.6250). We obtained similar results using CRISPR-mediated knockout of FIH in primary hippocampal cultures. Two different guide RNAs efficiently targeted FIH in primary cultures (Figure 5A). Both guides replicated the baseline increase in the frequency of Ca^{2+} transients observed with DM-NOFD (Figures 5B, C; *P* = 0.0029 and 0.0012, respectively). These cultures targeted for CRISPR-mediated FIH deletion also did not show a significant increase in neuronal activity in response to Trpa1 activation with AITC (Figures 5B, D; *P* > 0.05). Together, these observations suggest a physiological role for FIH and TRPA1 interaction in regulating neuronal activity patterns.

Discussion

Cellular and functional analyses suggest that TRPA1's sensitivity to AITC is linked to FIH-mediated hydroxylation of TRPA1 N336. The lack of effect by AITC on neuronal cultures treated with FIH inhibitor or with CRISPR-mediated deletion suggests that hydroxylation of TRPA1 is required for discernible channel function. This aligns with our observations in TRPA1-expressing HEK 293T cells: both exhibit a clear response to AITC. However, this response is diminished or delayed in TRPA1-expressing HEK 293T cells and absent in primary hippocampal cultures when FIH activity is lacking. However, the mechanisms connecting asparagine hydroxylation to TRPA1 function remain unclear. Further analyses will be required to assess whether the lack of function results from reduced cell surface localisation or impaired ion channel kinetics in non-hydroxylated TRPA1. The N-terminal cytosolic domain of TRPA1, which includes its ARD, is known to facilitate interactions with proteins such as calmodulin (43). Hydroxylation of asparagine residues within ARDs has been shown to stabilize the ARD fold (44), suggesting that TRP channel hydroxylation may influence the binding affinity of regulatory proteins. Phosphorylation of serine and threonine residues within the ARD has been reported to modulate TRPA1 sensitivity to AITC, likely by altering calcium influx (45). However, given the subtler nature of hydroxylation compared to phosphorylation, it may be considered unlikely that ARD hydroxylation will affect channel sensitivity through the same mechanism.

Interestingly, co-immunoprecipitation experiments imply that the L340R FIH variant, which is unable to dimerize (38), binds better with V5-TRPA1 than WT or catalytically impaired but dimeric D201A FIH (46). These observations suggest that TRPA1 binding to FIH may involve the FIH dimer interface. Crystallographic studies on FIH in complex with TRPA1 ARD fragments show active site cleft binding in a manner similar to that

of HIF-1α and previously studied ARD FIH substrates (10). FIH forms a homodimer in solution which can, at least in the crystal state, bind two substrates simultaneously (38). There is thus potential for the FIH dimer to simultaneously interact with two ARDs either from the same, or different, TRP channels. This potential for FIH to form dynamic complexes with two substrates which bind, but which may not both be hydroxylation substrates, brings further complexity to the cellular biochemistry of FIH. In addition, FIH has been shown to catalyse hydroxylation of multiple residues (including asparagine-, histidine- and aspartate-residues) on a wide range of ARD containing proteins (18-24, 47). Given the multiple cellular substrates of FIH, it is possible that some of the cellular observations linking FIH and TRPA1 channel function are indirectly mediated, potentially mediated by the effects of FIH on small-molecule redox related metabolism (25-29). In future work it will also be important to show that FIH-catalysed TRPA1 channel hydroxylation occurs under natural conditions; in this regard development of antibodies selective for Asn-hydroxylated TRP channels are of interest.

Despite the potential complexities, inhibiting FIH, either through use of a selective inhibitor or CRISPR-mediated knockout in primary hippocampal cultures, resulted in an increased baseline frequency of Ca^{2+} transients. These findings demonstrate that FIH activity plays a key role in regulating neuronal network activity in cultured neurons, highlighting the significant impact of FIH activity on neuronal excitability—an essential process for sensory processing and cognition. The observed changes in baseline activity may result from inhibiting the direct hydroxylation of TRPA1 by FIH, but FIH inhibition is likely to affect other ankyrin repeat domain (ARD) proteins including: voltage-gated ion channels, scaffolding proteins, cytoskeletal components, or synaptic regulators involved in neuronal excitability. Additionally, the increased frequency of

Ca^{2+} transients may represent a form of homeostatic plasticity, wherein neurons adjust their intrinsic excitability to maintain stable network function. Furthermore, alterations in HIF signaling could influence oxygen homeostasis and metabolism, indirectly shaping neuronal activity. To assess these mechanisms further work is required.

We recognize that TRPA1 expression is robust in sensory ganglia (2) but more controversial and likely lower in hippocampal neurons (3), which represents a limitation of our study. Nonetheless, our molecular and functional data support its presence and activity in hippocampal cultures, and even low-abundance ion channels can exert significant effects on network function. While DRG and trigeminal neurons remain the primary models for TRPA1 in nociception (2), hippocampal cultures provide complementary insight into potential central roles, such as stress responses and synaptic modulation. Future *in vivo* studies and cell-type–specific analyses will be needed to consolidate its contribution to neuronal physiology.

Experimental Procedures

Cell culture and reagents

WT and FIH KO 293T cells, generously provided by Prof. Sir Peter Ratcliffe and Dr. Ya-Min Tian (University of Oxford), were cultured in Dulbecco's Modified Eagle Medium (DMEM) (Invitrogen), supplied with 10% fetal bovine serum (FBS) (Sigma-Aldrich) and antibiotics as appropriate. All cells were cultured at 37 °C and 5% CO_2. Cells were transfected with the indicated plasmids using the Lipofectamine 3000 Transfection Reagent (Invitrogen) according to the manufacturer's instructions.

All experiments using primary murine cultures were performed in accordance with the Animals (Scientific Procedures) Act 1986 set out by the UK Home Office and approved by the University of Southampton Ethics Committee. For primary neuronal cultures, required brain regions or ganglia were isolated from E15-E18 C57BL/6 embryos and dissociated with 0.05% trypsin for 6-8 min at 37°C before quenching the trypsin with FBS. The solution was exchanged to culture medium (2% B27 supplement in phenol red-free neurobasal medium, 0.5 mM GlutaMax) and cells were dissociated by carefully pipetting 6-8 times. Cells were plated on poly-D-lysine coated dishes. For DRG cultures, media were further supplemented with 100 ng/ ml nerve growth factor (NGF). Neuronal cultures were transduced at day *in vitro* (DIV) 1 using indicated lentivirus (details provided in the Supplementary Materials). HC-030031 was from MedChemExpress (HY-15064).

Immunoprecipitation and western blot analysis

Western blot analyses were performed with lysates from cells lysed with urea buffer (8 M urea, 1 M thiourea, 0.5% CHAPS, 50 mM 1,4-dithiothreitol (DTT) and 24 mM spermine). The bound proteins were separated on sodium dodecyl sulphate (SDS)

polyacrylamide gels and subjected to immunoblotting with the indicated antibodies. For immunoprecipitations, cells were lysed for 30 min at 4 °C in 50 mm Tris/HCl (pH 7.5), 120 mm NaCl, 1 mm ethylenediaminetetraacetic acid (EDTA) and 0.1% Nonidet P-40 detergent (Sigma-Aldrich), with protease inhibitors (cOmplete™, EDTA-free Protease Inhibitor Cocktail, Roche). Anti-HA (Santa Cruz Biotechnology, sc-7392) or control antibodies and Protein G magnetic beads (Thermo Fisher Scientific) were added to the lysate for 16 h at 4 °C. Immunoprecipitates were washed 4 times with cold phosphate buffered saline (PBS) followed by the addition of SDS sample buffer. The bound proteins were separated on SDS polyacrylamide gels and subjected to immunoblotting with the indicated antibodies. Primary antibodies were from Cell Signaling Technology (β-Tubulin, 1:5000, 86298, mouse monoclonal; HA, 1:1000, 3724, rabbit monoclonal), Santa Cruz Biotechnology (GFP, 1:500, sc-9996, mouse monoclonal), Moravian Biotech (murine FIH, clone 3F9, 1:25; kindly provided by Prof. Xin Lu, University of Oxford) (35), human FIH (monoclonal 162 C; kindly provided by Prof. Sir Peter Ratcliffe, University of Oxford), Bio-Rad Laboratories (V5, 1:1000, MCA1360, mouse monoclonal) and Novus Biologicals (TRPA1, 1:500, NB110-40763, rabbit polyclonal). Signals were detected using an Odyssey imaging system (LI-COR) and evaluated by ImageJ 1.42q software (National Institutes of Health). Uncropped western blot images are provided in the Supplementary Materials.

RT-PCR

RNA was isolated from primary cultures using the RNeasy kit (QIAGEN) and 200ng RNA were reverse transcribed using oligo-dT primers and the Precision nanoScript 2 reverse transcription kit (Primer Design) according to the manufacturer's instructions. The resulting cDNA was analyzed by end-point PCR using RedTaq ReadyMix PCR

Reaction Mix (Sigma-Aldrich) and a GeneAmp PCR System 9700 (Applied Biosystems). The primers and PCR conditions are listed in Supplementary Table 1. Uncropped agarose gel images can be found in the Supplementary Materials.

Live cell imaging and analysis

Cells were plated on glass bottom dishes (WillCo Wells) and transfected with the indicated plasmids using Lipofectamine 3000 Transfection Reagent (Invitrogen) according to the manufacturer's instructions. GCaMP6s was a gift from the Douglas Kim & GENIE Project (Addgene plasmid # 40753; RRID:Addgene_40753). Prior to imaging, cells were switched into 1 ml phenol red-free DMEM supplemented with 20mM HEPES-NaOH pH 7.4 and imaged using an inverted fluorescence DeltaVision Elite microscope equipped with a temperature-controlled chamber maintained at 37˚C, 20x UPlanSApo objective (NA 0.75), SSI 7-band LED, UltimateFocus and a monochrome sCMOS camera, using SoftWoRks software v6. Images were taken every second for 5 minutes. After sampling the baseline fluorescence for 60 s, 1 ml (2x final concentration, 20 μM, in imaging media) AITC was added to the dish to allow immediate mixing while continuing acquisition for a further 4 min. As a control, 0.2% DMSO was used. HC-030031 (MedChemExpress, HY-15064), a well-characterized and selective TRPA1 antagonist, was used at 20 μM. Images were analysed by outlining cells in the final frames of the movie, measuring fluorescence intensity across all frames in the stack using ImageJ (NIH) and expressing it as F/F0.

Murine hippocampal neuronal cultures were transduced using lentivirus and imaged at DIV13-15. Images were taken every 200 ms as described above. Relative frequency was analysed as reported (48).

Statistical analysis and repeatability of experiments

Statistical analyses were performed using R (version 4.3.0) or GraphPad Prism version 10 (GraphPad Software Inc.). For primary cultures, imaging data were derived from at least 4 independent preparations, and each data point relates to one plate. Normality was evaluated using the D'Agostino-Pearson test. For two-group comparisons, Student's *t*-test was applied for parametric data, while the Mann-Whitney *U* test was used for non-parametric data. Multiple parametric comparisons were analysed using one- or two-way ANOVA followed by Tukey's post-hoc test, whereas the Kruskal-Wallis test with Dunnett's post-hoc test was utilized for non-parametric comparisons. Results were considered significant if $P < 0.05$.

Data Availability

The authors confirm that the data supporting the findings of this study are available within the article and its supporting information.

Acknowledgments—We are grateful to Prof. Sir Peter Ratcliffe and Dr. Ya-Min Tian (University of Oxford) for providing the WT and FIH KO 293T cells, as well as the human FIH monoclonal antibody (162C), and to Prof. Xin Lu (University of Oxford) for the murine FIH antibody (clone 3F9). The authors also gratefully acknowledge the Imaging and Microscopy Centre at the Biological Sciences (University of Southampton) for their support and assistance in this work. For the purpose of open access, the authors have applied a CC-BY public copyright license to any Author Accepted Manuscript version arising from this submission.

Author contributions—T.G., D.M.L., S.W., L.Y., X.L. and E.R.D. investigation; Y.W., K.D. and C.J.S. writing–original draft; M.V.C. and N.D. writing–review & editing; C.J.S., M.V.C. and N.D. Resources; Y.W., K.D., M.V.C. and N.D. supervision; Y.W. project administration; Y.W. funding acquisition; T.G., D.M.L., S.W., L.Y., M.V.C., Y.W. and K.D. formal analysis; Y.W. and K.D. conceptualization.

Funding and additional information—Y.W. was supported by the UK Medical Research Council (MR/S025480/1) and a UK Academy of Medical Sciences/the Wellcome Trust Springboard Award (SBF002\1038). T.G., S.W. and L.Y. were supported by China Scholarship Council. N.D. acknowledges funding from the UK Biotechnology and Biological Sciences Research Council (BB/P003508/1 and BB/N016823/1). C.J.S thanks the BBSRC, Cancer Research UK, the Wellcome Trust for funding.

Conflict of interest—The authors declare that they have no conflicts of interest with the contents of the article.

Abbreviations—The abbreviations used are: FIH, factor inhibiting hypoxia inducible factor; TRPA1, transient receptor potential cation channel, subfamily A, member 1; AITC, allyl isothiocyanate; PHD, Prolyl Hydroxylase Domain protein; ARD, ankyrin repeat domain; CAD, C-terminal activation domain; WT, wild-type; DM-NOFD, dimethyl *N*-oxalyl-*D*-phenylalanine

Figure legends

Figure 1. TRPA1 binding to FIH involves the dimer interface. *A*, Total cell lysates from FIH KO 293T cells transfected with the indicated plasmids were immunoprecipitated (IP) with an anti-HA antibody. V5-TRPA1 and HA-FIH levels are indicated. β-Tubulin was used as a loading control. *B*, Graph showing protein levels of pulled-down V5-TRPA1 normalized to the total level of V5-TRPA1 in whole cell lysates. Data are means ± SD (standard deviation) with *P* values by Dunnett's multiple comparisons test.

Figure 2. Effects of FIH-mediated hydroxylation of TRPA1 on AITC-induced channel activation in TRPA1-expressed HEK 293T cells. A, Total cell lysates from WT or FIH KO 293T cells transfected with the indicated plasmids were collected. V5-TRPA1, GCaMP (GFP) and FIH levels are indicated; β-tubulin was used as a loading control. B, Time-course of responses of WT or FIH KO 293T cells transfected with indicated plasmids to addition of allyl isothiocyanate (AITC, 20 μM) (arrows indicate addition points). Relative changes in GCaMP fluorescent levels are shown. Data are mean ± SEM (standard error of the mean).

Figure 3. Effects of DMSO and AITC in the absence or presence of HC-030031 on GCaMP fluorescence in murine hippocampal cultures. A, Gene expression levels of FIH (*Hif1an*) and *Trpa1* in the indicated murine primary cultures. β-actin (*Actb*) was used as a loading control. DRG: dorsal root ganglion. B-D, Representative traces and graphs showing GCaMP fluorescent levels in murine hippocampal cultures with the indicated treatment. AITC was applied at 20 μM, with 0.2% DMSO serving as the control. HC-030031, a selective and well-characterized TRPA1 antagonist, was used at 20 μM. Data are presented as mean ± SD, and statistical significance was assessed using a two-tailed paired t-test. ns: not significant.

Figure 4. Effects of FIH inhibition using DM-NOFD on AITC-induced channel activation in murine hippocampal cultures. A, Representative traces of GCaMP fluorescent levels in murine hippocampal cultures with the indicated treatment. B, Graph showing frequency (peaks/min) of GCaMP fluorescent levels in murine

hippocampal cultures with the indicated treatment. AITC was applied at 20 μM. Data are mean ± SD with *P* values by Tukey's multiple comparisons test.

Figure 5. Effects of FIH deletion using CRISPR gene editing on AITC-induced channel activation in murine hippocampal cultures. A, FIH and Trpa1 levels in total cell lysates from control or FIH-deleted murine primary hippocampal cultures using CRISPR gene editing; β-tubulin was used as a loading control. B, Representative traces of GCaMP fluorescent levels in murine hippocampal cultures with the indicated treatment. C and D, Graphs showing frequency (peaks/min) of GCaMP fluorescent levels in murine hippocampal cultures with the indicated treatment. AITC was applied at 20 μM. Data are mean ± SD with *P* values by Dunnett's (C) or Tukey's (D) multiple comparisons test. ns: not significant.

References

1. Hardie, R. C., and Minke, B. (1992) The trp gene is essential for a light-activated Ca2+ channel in Drosophila photoreceptors *Neuron* **8**, 643-651

2. Kashio, M., and Tominaga, M. (2022) TRP channels in thermosensation *Curr Opin Neurobiol* **75**, 102591

3. de Moura, J. C., Noroes, M. M., Rachetti Vde, P., Soares, B. L., Preti, D., Nassini, R. *et al.* (2014) The blockade of transient receptor potential ankirin 1 (TRPA1) signalling mediates antidepressant- and anxiolytic-like actions in mice *Br J Pharmacol* **171**, 4289-4299

4. Kawabata, R., Shimoyama, S., Ueno, S., Yao, I., Arata, A., and Koga, K. (2023) TRPA1 as a O(2) sensor detects microenvironmental hypoxia in the mice anterior cingulate cortex *Sci Rep* **13**, 2960

5. Zhao, J., Lin King, J. V., Paulsen, C. E., Cheng, Y., and Julius, D. (2020) Irritant-evoked activation and calcium modulation of the TRPA1 receptor *Nature* **585**, 141-145

6. Hinman, A., Chuang, H. H., Bautista, D. M., and Julius, D. (2006) TRP channel activation by reversible covalent modification *Proc Natl Acad Sci U S A* **103**, 19564-19568

7. Takahashi, N., Kuwaki, T., Kiyonaka, S., Numata, T., Kozai, D., Mizuno, Y. *et al.* (2011) TRPA1 underlies a sensing mechanism for O2 *Nat Chem Biol* **7**, 701-711

8. Bessac, B. F., Sivula, M., von Hehn, C. A., Escalera, J., Cohn, L., and Jordt, S. E. (2008) TRPA1 is a major oxidant sensor in murine airway sensory neurons *J Clin Invest* **118**, 1899-1910

9. Cockman, M. E., Lippl, K., Tian, Y. M., Pegg, H. B., Figg, W. D. J., Abboud, M. I. *et al.* (2019) Lack of activity of recombinant HIF prolyl hydroxylases (PHDs) on reported non-HIF substrates *Elife* **8**, e46490

10. Saward, B. G., Leissing, T. M., Clifton, I. J., Tumber, A., Timperley, C. M., Hopkinson, R. J. *et al.* (2023) Biochemical and Structural Insights into FIH-Catalysed Hydroxylation of Transient Receptor Potential Ankyrin Repeat Domains *Chembiochem* **24**, e202200576

11. Mahon, P. C., Hirota, K., and Semenza, G. L. (2001) FIH-1: a novel protein that interacts with HIF-1alpha and VHL to mediate repression of HIF-1 transcriptional activity *Genes Dev* **15**, 2675-2686

12. Lando, D., Peet, D. J., Gorman, J. J., Whelan, D. A., Whitelaw, M. L., and Bruick, R. K. (2002) FIH-1 is an asparaginyl hydroxylase enzyme that regulates the transcriptional activity of hypoxia-inducible factor *Genes Dev* **16**, 1466-1471

13. Lando, D., Peet, D. J., Whelan, D. A., Gorman, J. J., and Whitelaw, M. L. (2002) Asparagine hydroxylation of the HIF transactivation domain a hypoxic switch *Science* **295**, 858-861

14. Hewitson, K. S., McNeill, L. A., Riordan, M. V., Tian, Y. M., Bullock, A. N., Welford, R. W. *et al.* (2002) Hypoxia-inducible factor (HIF) asparagine hydroxylase is identical to factor inhibiting HIF (FIH) and is related to the cupin structural family *J Biol Chem* **277**, 26351-26355

15. Elkins, J. M., Hewitson, K. S., McNeill, L. A., Seibel, J. F., Schlemminger, I., Pugh, C. W. *et al.* (2003) Structure of factor-inhibiting hypoxia-inducible factor (HIF) reveals mechanism of oxidative modification of HIF-1 alpha *J Biol Chem* **278**, 1802-1806

16. McNeill, L. A., Hewitson, K. S., Claridge, T. D., Seibel, J. F., Horsfall, L. E., and Schofield, C. J. (2002) Hypoxia-inducible factor asparaginyl hydroxylase (FIH-1) catalyses hydroxylation at the beta-carbon of asparagine-803 *Biochem J* **367**, 571-575

17. Wang, Y., Zhong, S., Schofield, C. J., Ratcliffe, P. J., and Lu, X. (2018) Nuclear entry and export of FIH are mediated by HIF1alpha and exportin1, respectively *J Cell Sci* **131**,

18. Coleman, M. L., McDonough, M. A., Hewitson, K. S., Coles, C., Mecinovic, J., Edelmann, M. *et al.* (2007) Asparaginyl hydroxylation of the Notch ankyrin repeat domain by factor inhibiting hypoxia-inducible factor *J Biol Chem* **282**, 24027-24038

19. Zheng, X., Linke, S., Dias, J. M., Gradin, K., Wallis, T. P., Hamilton, B. R. *et al.* (2008) Interaction with factor inhibiting HIF-1 defines an additional mode of cross-coupling between the Notch and hypoxia signaling pathways *Proceedings of the National Academy of Sciences of the United States of America* **105**, 3368-3373

20. Janke, K., Brockmeier, U., Kuhlmann, K., Eisenacher, M., Nolde, J., Meyer, H. E. *et al.* (2013) Factor inhibiting HIF-1 (FIH-1) modulates protein interactions of apoptosis-stimulating p53 binding protein 2 (ASPP2) *J Cell Sci* **126**, 2629-2640

21. Cockman, M. E., Webb, J. D., Kramer, H. B., Kessler, B. M., and Ratcliffe, P. J. (2009) Proteomics-based identification of novel factor inhibiting hypoxia-inducible factor (FIH) substrates indicates widespread asparaginyl hydroxylation of ankyrin repeat domain-containing proteins *Mol Cell Proteomics* **8**, 535-546

22. Karttunen, S., Duffield, M., Scrimgeour, N. R., Squires, L., Lim, W. L., Dallas, M. L. *et al.* (2015) Oxygen-dependent hydroxylation by FIH regulates the TRPV3 ion channel *J Cell Sci* **128**, 225-231

23. Cockman, M. E., Lancaster, D. E., Stolze, I. P., Hewitson, K. S., McDonough, M. A., Coleman, M. L. *et al.* (2006) Posttranslational hydroxylation of ankyrin repeats in IkappaB proteins by the hypoxia-inducible factor (HIF) asparaginyl hydroxylase, factor inhibiting HIF (FIH) *Proc Natl Acad Sci U S A* **103**, 14767-14772

24. Leissing, T. M., Hardy, A. P., Chan, H., Wang, Y., Tumber, A., Chowdhury, R. *et al.* (2022) Factor inhibiting HIF can catalyze two asparaginyl hydroxylations in VNVN motifs of ankyrin fold proteins *J Biol Chem* **298**, 102020

25. Zhang, N., Fu, Z., Linke, S., Chicher, J., Gorman, J. J., Visk, D. *et al.* (2010) The asparaginyl hydroxylase factor inhibiting HIF-1alpha is an essential regulator of metabolism *Cell Metab* **11**, 364-378

26. Scholz, C. C., Rodriguez, J., Pickel, C., Burr, S., Fabrizio, J. A., Nolan, K. A. *et al.* (2016) FIH Regulates Cellular Metabolism through Hydroxylation of the Deubiquitinase OTUB1 *PLoS Biol* **14**, e1002347

27. Peng, H., Hamanaka, R. B., Katsnelson, J., Hao, L. L., Yang, W., Chandel, N. S. *et al.* (2012) MicroRNA-31 targets FIH-1 to positively regulate corneal epithelial glycogen metabolism *FASEB J* **26**, 3140-3147

28. Sim, J., Cowburn, A. S., Palazon, A., Madhu, B., Tyrakis, P. A., Macias, D. *et al.* (2018) The Factor Inhibiting HIF Asparaginyl Hydroxylase Regulates Oxidative Metabolism and Accelerates Metabolic Adaptation to Hypoxia *Cell Metab* **27**, 898-913 e897

29. Wu, Y., Chen, Y., Corner, T. P., Nakashima, Y., Salah, E., Li, Z. *et al.* (2024) A Small-Molecule Inhibitor of Factor Inhibiting HIF Binding to a Tyrosine-Flip Pocket for the Treatment of Obesity *Angew Chem Int Ed Engl* **63**, e202410438

30. Peng, H., Kaplan, N., Hamanaka, R. B., Katsnelson, J., Blatt, H., Yang, W. *et al.* (2012) microRNA-31/factor-inhibiting hypoxia-inducible factor 1 nexus regulates keratinocyte differentiation *Proc Natl Acad Sci U S A* **109**, 14030-14034

31. Kiriakidis, S., Henze, A. T., Kruszynska-Ziaja, I., Skobridis, K., Theodorou, V., Paleolog, E. M. *et al.* (2015) Factor-inhibiting HIF-1 (FIH-1) is required for human vascular endothelial cell survival *FASEB J* **29**, 2814-2827

32. Brereton, C. J., Yao, L., Davies, E. R., Zhou, Y., Vukmirovic, M., Bell, J. A. *et al.* (2022) Pseudohypoxic HIF pathway activation dysregulates collagen structure-function in human lung fibrosis *Elife* **11**,

33. Pelletier, J., Dayan, F., Durivault, J., Ilc, K., Pecou, E., Pouyssegur, J. *et al.* (2012) The asparaginyl hydroxylase factor-inhibiting HIF is essential for tumor growth through suppression of the p53-p21 axis *Oncogene* **31**, 2989-3001

34. Kuzmanov, A., Wielockx, B., Rezaei, M., Kettelhake, A., and Breier, G. (2012) Overexpression of factor inhibiting HIF-1 enhances vessel maturation and tumor growth via platelet-derived growth factor-C *Int J Cancer* **131**, E603-613

35. Ma, J., Al Moussawi, K., Lou, H., Chan, H. F., Wang, Y., Chadwick, J. *et al.* (2024) Deficiency of factor-inhibiting HIF creates a tumor-promoting immune microenvironment *Proc Natl Acad Sci U S A* **121**, e2309957121

36. Kang, J., Shin, S. H., Yoon, H., Huh, J., Shin, H. W., Chun, Y. S. *et al.* (2017) FIH is an oxygen sensor in ovarian cancer for G9a/GLP-driven epigenetic regulation of metastasis-related genes *Cancer research* 10.1158/0008-5472.CAN-17-2506

37. Rodriguez, J., Pilkington, R., Garcia Munoz, A., Nguyen, L. K., Rauch, N., Kennedy, S. *et al.* (2016) Substrate-Trapped Interactors of PHD3 and FIH Cluster in Distinct Signaling Pathways *Cell Rep* **14**, 2745-2760

38. Lancaster, D. E., McNeill, L. A., McDonough, M. A., Aplin, R. T., Hewitson, K. S., Pugh, C. W. *et al.* (2004) Disruption of dimerization and substrate phosphorylation inhibit factor inhibiting hypoxia-inducible factor (FIH) activity *Biochem J* **383**, 429-437

39. Raisinghani, M., Zhong, L., Jeffry, J. A., Bishnoi, M., Pabbidi, R. M., Pimentel, F. *et al.* (2011) Activation characteristics of transient receptor potential ankyrin 1 and its role in nociception *American Journal of Physiology-Cell Physiology* **301**, C587-C600

40. Nakai, J., Ohkura, M., and Imoto, K. (2001) A high signal-to-noise Ca2+ probe composed of a single green fluorescent protein *Nature Biotechnology* **19**, 137-141

41. Gupta, R., Saito, S., Mori, Y., Itoh, S. G., Okumura, H., and Tominaga, M. (2016) Structural basis of TRPA1 inhibition by HC-030031 utilizing species-specific differences *Sci Rep* **6**, 37460

42. McDonough, M. A., McNeill, L. A., Tilliet, M., Papamicael, C. A., Chen, Q. Y., Banerji, B. *et al.* (2005) Selective inhibition of factor inhibiting hypoxia-inducible factor *J Am Chem Soc* **127**, 7680-7681

43. Singh, A. K., McGoldrick, L. L., Twomey, E. C., and Sobolevsky, A. I. (2018) Mechanism of calmodulin inactivation of the calcium-selective TRP channel TRPV6 *Science Advances* **4**, eaau6088

44. Kelly, L., McDonough, M. A., Coleman, M. L., Ratcliffe, P. J., and Schofield, C. J. (2009) Asparagine beta-hydroxylation stabilizes the ankyrin repeat domain fold *Mol Biosyst* **5**, 52-58

45. Hall, B. E., Prochazkova, M., Sapio, M. R., Minetos, P., Kurochkina, N., Binukumar, B. K. *et al.* (2018) Phosphorylation of the Transient Receptor Potential Ankyrin 1 by Cyclin-dependent Kinase 5 affects Chemo-nociception *Scientific Reports* **8**, 1177

46. Hewitson, K. S., Holmes, S. L., Ehrismann, D., Hardy, A. P., Chowdhury, R., Schofield, C. J. *et al.* (2008) Evidence that two enzyme-derived histidine ligands are sufficient for iron binding and catalysis by factor inhibiting HIF (FIH) *J Biol Chem* **283**, 25971-25978

47. Chowdhury, R., Leung, I. K., Tian, Y. M., Abboud, M. I., Ge, W., Domene, C. *et al.* (2016) Structural basis for oxygen degradation domain selectivity of the HIF prolyl hydroxylases *Nat Commun* **7**, 12673

48. Sun, Z., and Sudhof, T. C. (2021) A simple Ca(2+)-imaging approach to neural network analyses in cultured neurons *J Neurosci Methods* **349**, 109041

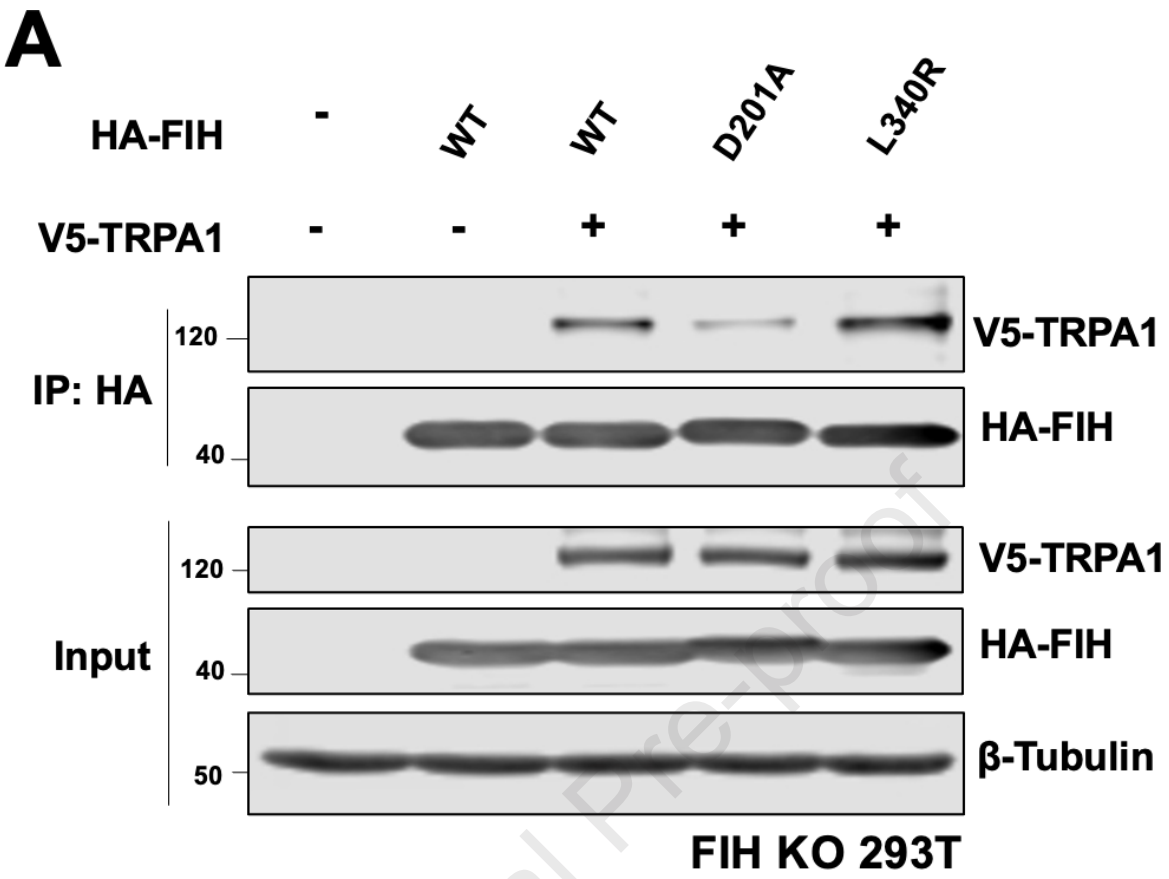

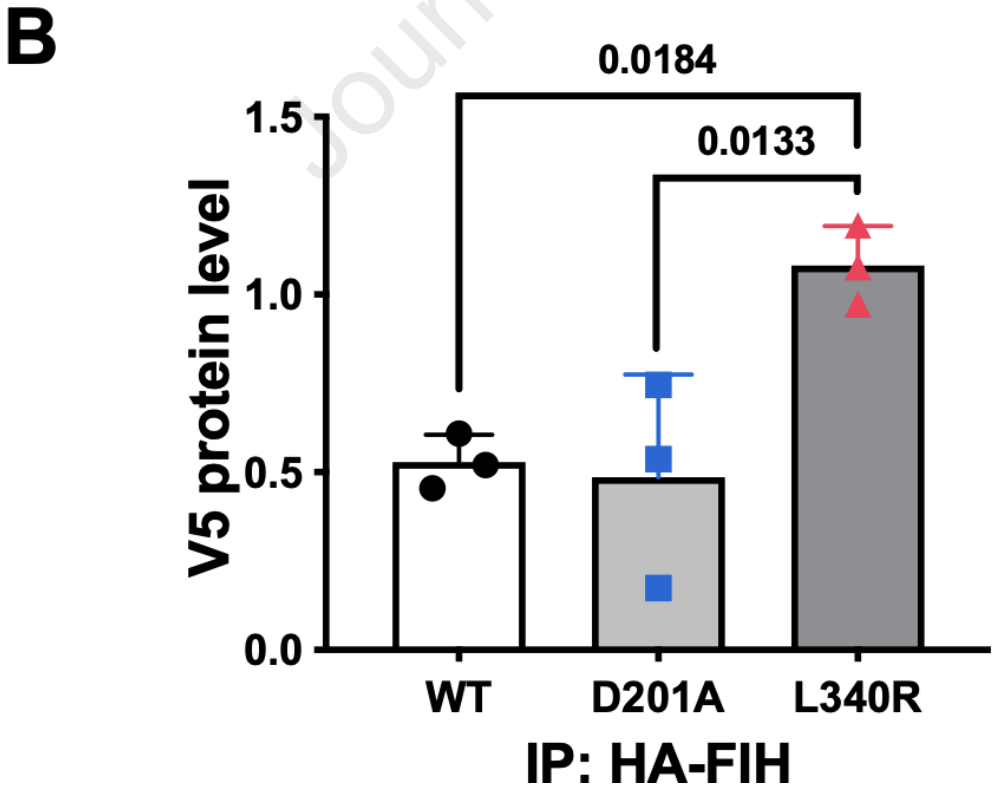

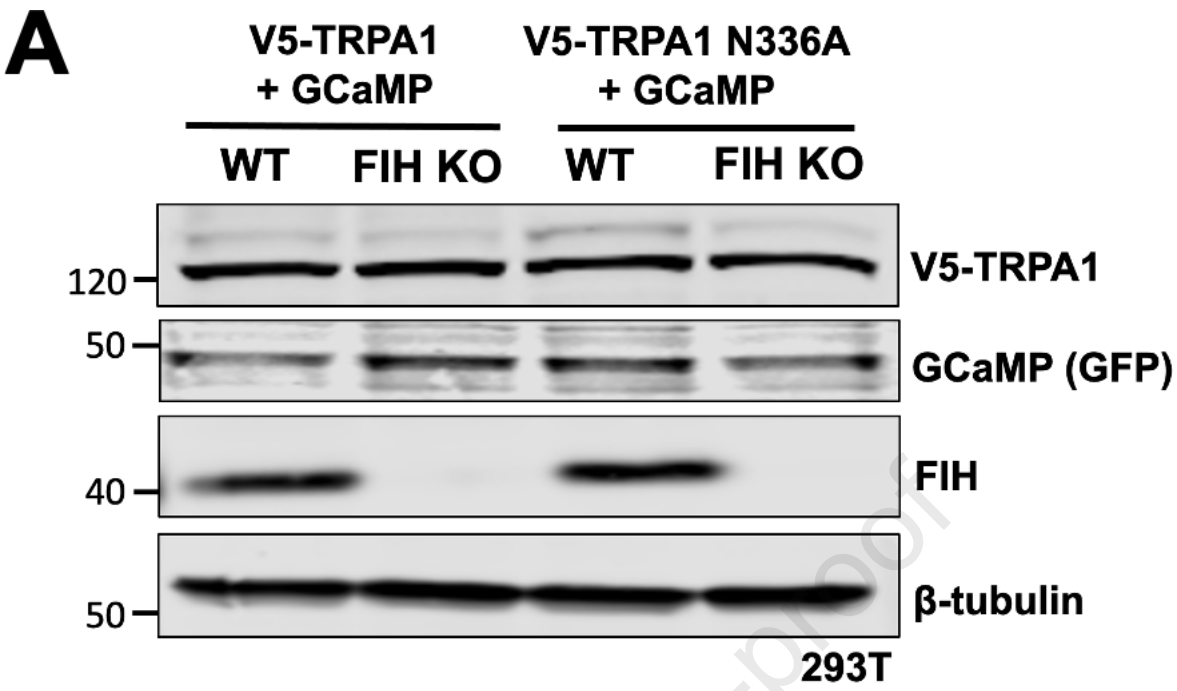

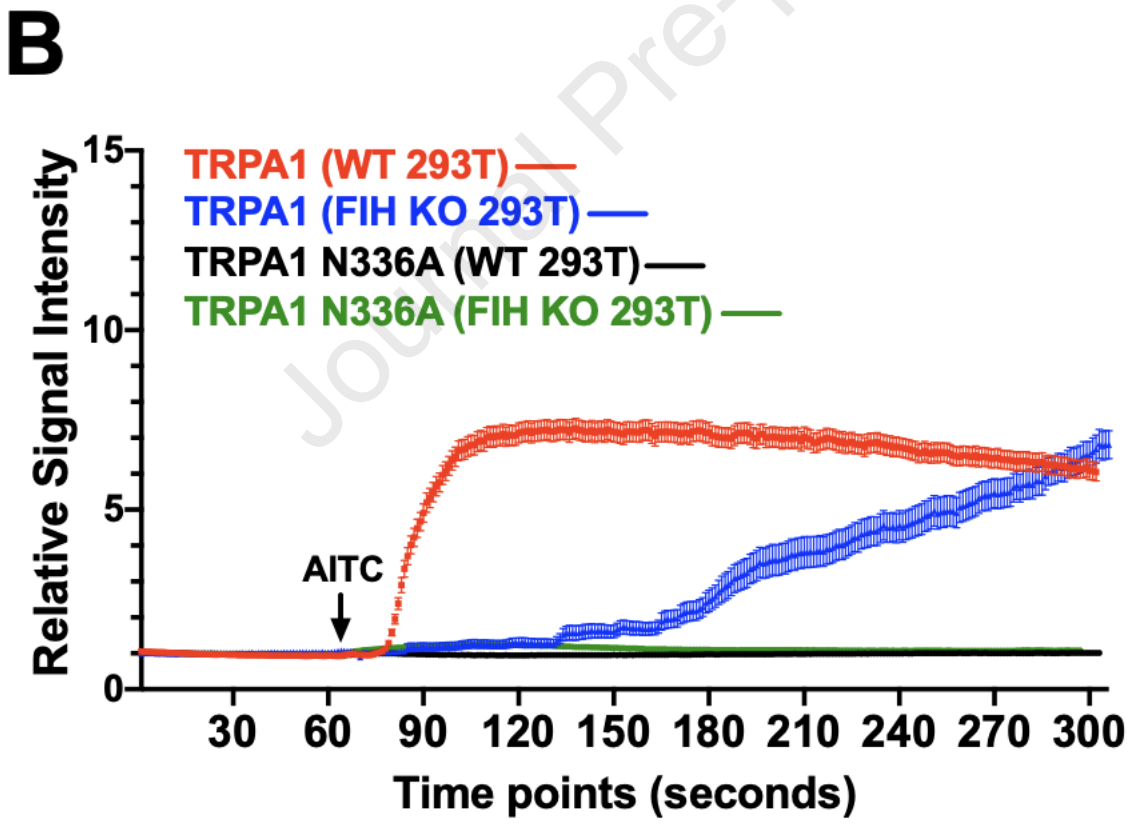

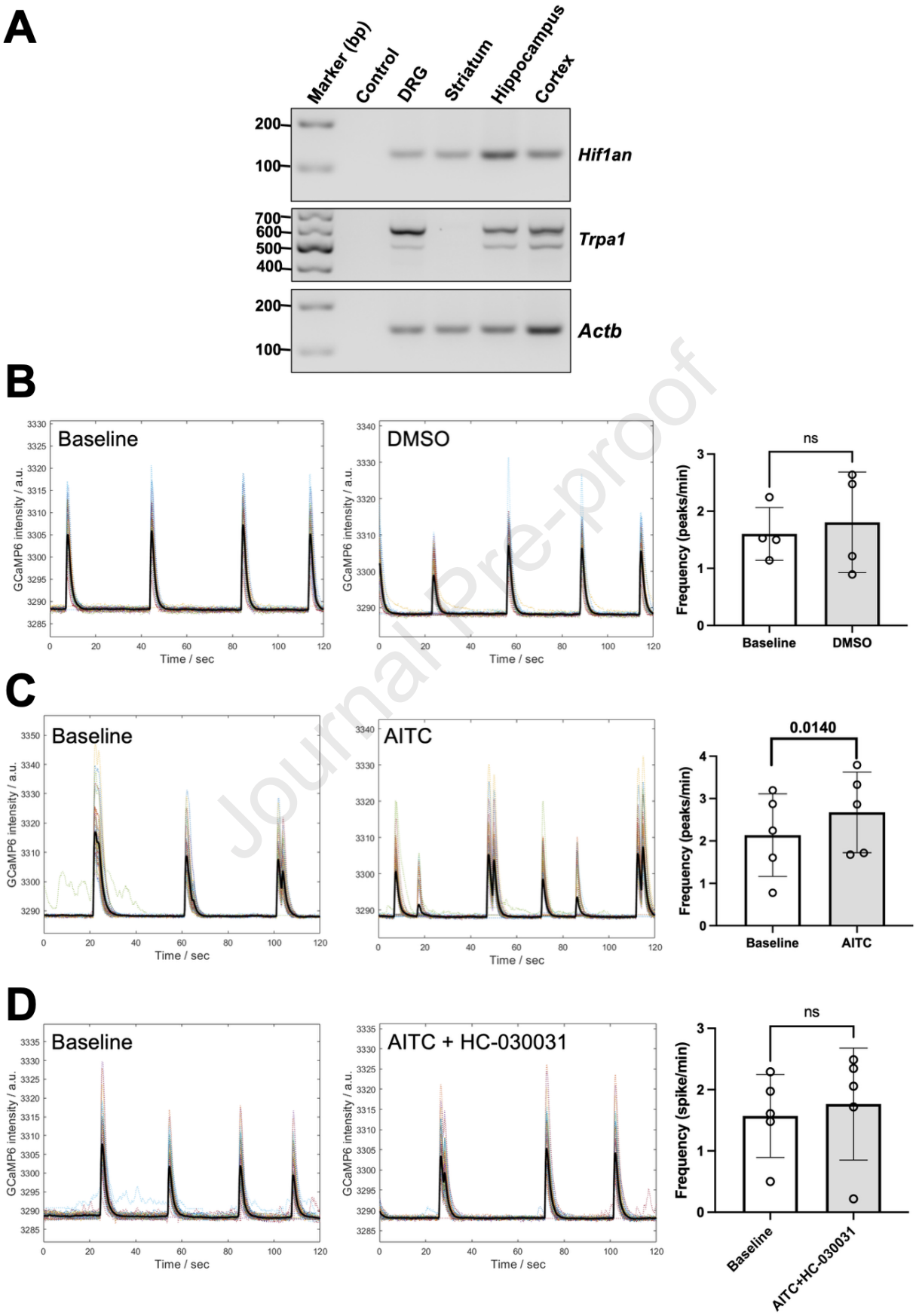

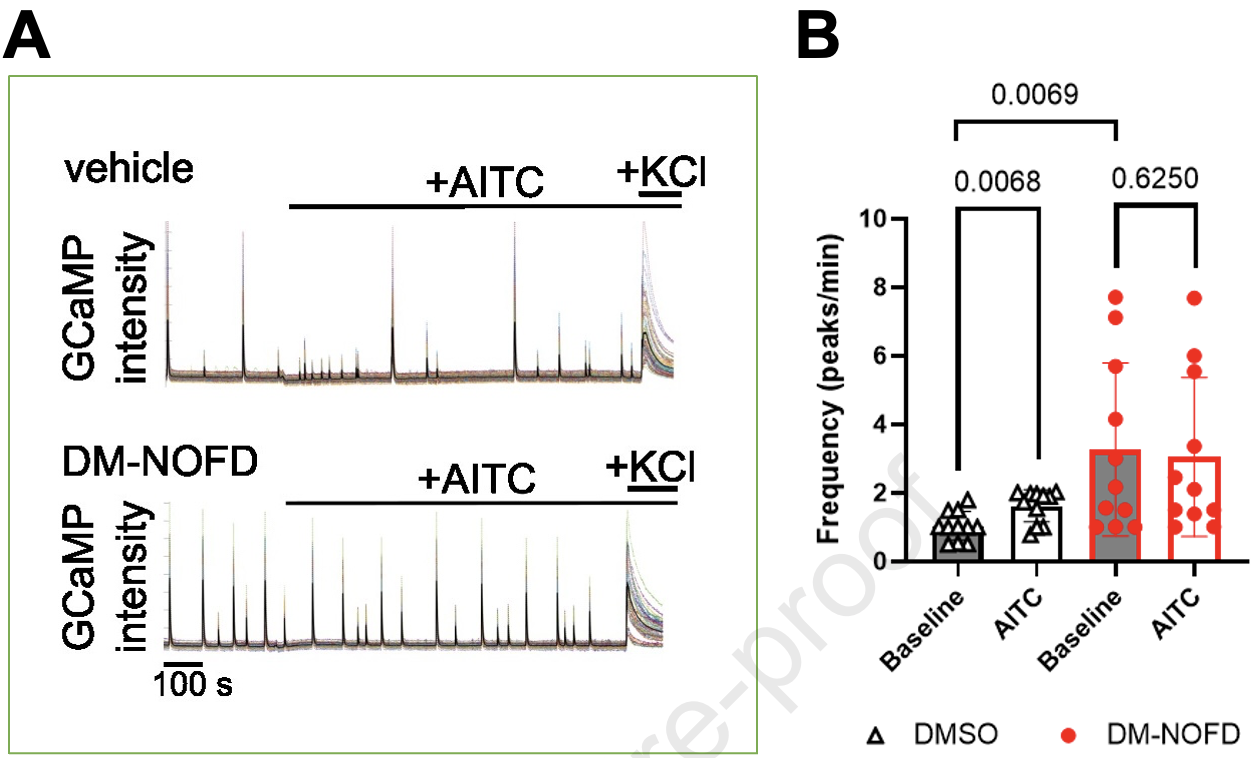

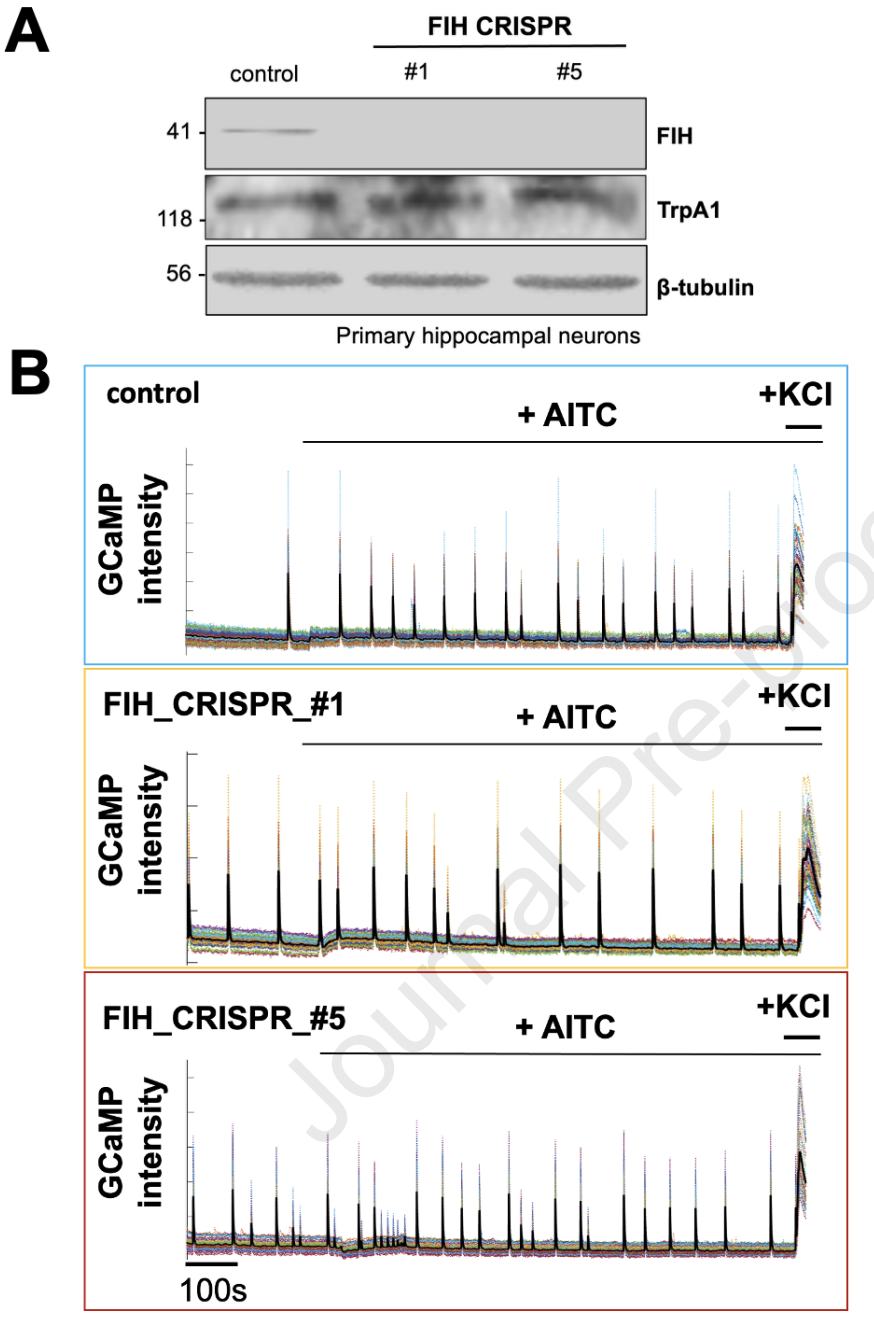

Declaration of Interest Statement

☒ The authors declare that they have no known competing financial interests or personal relationships that could have appeared to influence the work reported in this paper.

☐ The author is an Editorial Board Member/Editor-in-Chief/Associate Editor/Guest Editor for this journal and was not involved in the editorial review or the decision to publish this article.

☐ The authors declare the following financial interests/personal relationships which may be considered as potential competing interests: